European Journal of Radiology 85 (2016) 1574–1580

Contents lists available at ScienceDirect

European Journal of Radiology

journal homepage: www.elsevier.com/locate/ejrad

Dual-energy CT to estimate clinical severity of chronic thromboembolic pulmonary hypertension: Comparison with invasive right heart catheterization

Hidenobu Takagi[a], Hideki Ota[a,*], Koichiro Sugimura[b], Katharina Otani[c], Junya Tominaga[a], Tatsuo Aoki[b], Shunsuke Tatebe[b], Masanobu Miura[b], Saori Yamamoto[b], Haruka Sato[b], Nobuhiro Yaoita[b], Hideaki Suzuki[b], Hiroaki Shimokawa[b], Kei Takase[a]

[a] Department of Diagnostic Radiology, Tohoku University Hospital, 1-1, Seiryo-machi, Aoba-ku, Sendai, Miyagi, #980-8574, Japan
[b] Department of Cardiovascular Medicine, Tohoku University Hospital, 1-1, Seiryo-machi, Aoba-ku, Sendai, Miyagi, #980-8574, Japan
[c] Diagnostic Imaging Business Area, DI Research & Collaboration Department, Siemens Healthcare KK, Gate City Osaki West Tower, 1-11-1, Osaki, Shinagawa-ku, Tokyo, #141-8644, Japan

ARTICLE INFO

Article history:
Received 11 February 2016
Received in revised form 13 May 2016
Accepted 15 June 2016

Keywords:
Dual-energy CT (DE-CT)
Lung perfused blood volume (Lung PBV)
Chronic thromboembolic pulmonary hypertension (CTEPH)
Pulmonary hypertension (PH)

ABSTRACT

Purpose: To evaluate whether the extent of perfusion defects assessed by examining lung perfused blood volume (PBV) images is a stronger estimator of the clinical severity of chronic thromboembolic pulmonary hypertension (CTEPH) compared with other computed tomography (CT) findings and noninvasive parameters.

Materials and methods: We analyzed 46 consecutive patients (10 men, 36 women) with CTEPH who underwent both dual-energy CT and right-heart catheter (RHC) examinations. Lung PBV images were acquired using a second-generation dual-source CT scanner. Two radiologists independently scored the extent of perfusion defects in each lung segment employing the following criteria: 0, no defect, 1, defect in <50% of a segment, 2, defect in ≥50% of a segment. Each lung PBV score was defined as the sum of the scores of 18 segments. In addition, all of the following were recorded: 6-min walk distance (6MWD), brain natriuretic peptide (BNP) level, and RHC hemodynamic parameters including pulmonary artery pressure (PAP), right ventricular pressure (RVP), cardiac output (CO), the cardiac index (CI), and pulmonary vascular resistance (PVR). Bootstrapped weighted kappa values with 95% confidence intervals (CIs) were calculated to evaluate the level of interobserver agreement. Correlations between lung PBV scores and other parameters were evaluated by calculating Spearman's rho correlation coefficients. Multivariable linear regression analyses (using a stepwise method) were employed to identify useful estimators of mean PAP and PVR among CT, BNP, and 6MWD parameters. A p value < 0.05 was considered to reflect statistical significance.

Results: Interobserver agreement in terms of the scoring of perfusion defects was excellent ($\kappa = 0.88$, 95% CIs: 0.85, 0.91). The lung PBV score was significantly correlated with the PAP (mean, rho = 0.48; systolic, rho = 0.47; diastolic, rho = 0.39), PVR (rho = 0.47), and RVP (rho = 0.48) (all p values < 0.01). Multivariable linear regression analyses showed that only the lung PBV score was significantly associated with both the mean PAP (coefficient, 0.84, $p < 0.01$) and the PVR (coefficient, 28.83, $p < 0.01$).

Conclusion: The lung PBV score is a useful and noninvasive estimator of clinical CTEPH severity, especially in comparison with the mean PAP and PVR, which currently serve as the gold standards for the management of CTEPH .

* Corresponding author.
E-mail addresses: hdnb69tkg@gmail.com (H. Takagi), h-ota@rad.med.tohoku.ac.jp (H. Ota), ksugimura@cardio.med.tohoku.ac.jp (K. Sugimura), katharina.otani@siemens.com (K. Otani), jrtomi@jf6.so-net.ne.jp (J. Tominaga), aokitatsuo@gmail.com (T. Aoki), shuntatebe@cardio.med.tohoku.ac.jp (S. Tatebe), masa-miura@cardio.med.tohoku.ac.jp (M. Miura), yamamoto@cardio.med.tohoku.ac.jp (S. Yamamoto), haruka.s@cardio.med.tohoku.ac.jp (H. Sato), tohokuyaoita@cardio.med.tohoku.ac.jp (N. Yaoita), hd.suzuki.1870031@cardio.med.tohoku.ac.jp (H. Suzuki), shimo@cardio.med.tohoku.ac.jp (H. Shimokawa), ktakase@rad.med.tohoku.ac.jp (K. Takase).

http://dx.doi.org/10.1016/j.ejrad.2016.06.010
0720-048X/

1. Introduction

Chronic thromboembolic pulmonary hypertension (CTEPH) develops in 2–4% of patients with acute pulmonary embolisms [1,2]. Deposition of thromboembolic materials obstructs the pulmonary vascular bed [3], triggering vasoconstriction and vascular remodeling [4]. Progressive pulmonary hypertension (mean pulmonary arterial pressure [PAP] ≥ 25 mmHg) combined with increased pulmonary vascular resistance (PVR) causes right-side cardiac failure. The prognosis of CTEPH patients is poor without treatment: the 2-year survival rate is 20% for those with a mean PAP > 50 mmHg and the 5-year survival rate 30% for those with a mean PAP > 30 mmHg [5,6]. However, pulmonary endarterectomy (PEA) [7] and (recently introduced) balloon pulmonary angioplasty (BPA) [8], combined with optimal medications, have improved prognosis. It is obviously necessary to evaluate CTEPH severity when seeking to predict prognosis and when contemplating therapeutic decisions. The 6-min walk distance (6MWD) [9] and the brain natriuretic peptide (BNP) level [10] are commonly used as noninvasive measures of the severity of pulmonary hypertension. However, the 6MWD is influenced by other physical conditions, and BNP levels are influenced by age, gender, and the assay system employed [11]. Invasive right-side heart catheter (RHC) examination is the gold standard used to diagnose the presence and evaluate the severity of CTEPH [12]; the procedure remains associated with risks of morbidity and mortality [13].

In terms of imaging modalities, radionuclide ventilation/perfusion (VQ) scanning has been recommended as a useful screen for CTEPH [12]. However, such scans have not been used to evaluate the clinical severity of CTEPH . CT pulmonary angiography (CTPA) is widely used both to diagnose CTEPH and to screen for other cardiopulmonary abnormalities [14]. The sensitivities of CTPA used to diagnose CTEPH were reported as 86–98% in recent studies [15,16]. In recent years, dual-energy computed tomography (DE-CT) has emerged as a promising tool for lung imaging. This scan mode allows the simultaneous acquisition of two datasets, one at low and one at high tube voltage. These datasets are post-processed to generate 120 kV gray-scale images and color-coded overlays highlighting the locations of the imaging material of choice (e.g., xenon or iodine) [17]. The lung PBV imaging reveals the distribution of intravenously injected iodine contrast material in the parenchyma. In CTEPH patients, the areas of concern in lung PBV images correspond well to such areas evident on pulmonary perfusion scintigraphs [18]. Because persistent macrovascular obstruction, vasoconstriction, and arteriopathy are considered to be fundamental in terms of the development of pulmonary hypertension in CTEPH patients [4,19], we hypothesized that the extent of hypoperfusion of the pulmonary arterial system, as reflected in color-coded lung PBV images, might indicate the clinical severity of CTEPH . However, few studies have tested the potential correlations between lung PBV findings and the clinical severity of disease [27,28].

We evaluated whether the extent of perfusion defects evident on lung PBV imaging better estimates the clinical severity of CTEPH compared to other CT and noninvasive parameters.

2. Materials and methods

This prospective study was approved by our local ethics committee, and written informed consent was obtained from all of the patients.

2.1. Patients

Fifty-two patients who underwent both DE-CT and RHC examinations between April 2014 and July 2015 were enrolled. Six patients for whom DE-CT and RHC examinations had been conducted more than 2 weeks apart were excluded because the clinical severity of the disease might have changed between examinations. The remaining 46 patients (10 men, 36 women; mean age 69 years [range: 21–81 years]) were included in further analyses. All of the patients were diagnosed as CTEPH by experienced cardiologists at our institution based on Nice guidelines [12]. Thirty-eight (82.6%) patients had been diagnosed with CTEPH before the study commenced; their DE-CT and RHC examinations were preoperative work-ups or postoperative follow-ups. The remaining eight (17.4%) CTEPH patients underwent both examinations for diagnostic purposes. All patients had been managed with medications including anticoagulants, diuretics, and vasodilators. Patient demographic characteristics and the interventions performed are summarized in Table 1.

Table 1
Patients' characteristics.

Number of patients	46
Sex	Men, 10 (21.7%), women, 36 (78.3%)
Age	Median, 69, range (21–81)
BMI	Median, 24.9, range (19.4–34.6)
Clinical diagnosis	CTEPH
Cardiopulmonary comorbidities	None
WHO-FC	I (n = 9), II (n = 33), III (n = 3), IV (n = 1)
Prior therapy	Medication only (n = 12)
	Medication with PEA (n = 1)
	Medication with BPA (n = 33)

BMI = body mass index, CTEPH = chronic thromboembolic pulmonary hypertension, WHO-FC = World Health Organization functional class, PEA = pulmonary endarterectomy, BPA = balloon pulmonary angioplasty.

2.2. CT acquisition protocol

Dual-energy CT data were acquired using a second-generation dual-source CT scanner (SOMATOM Definition Flash; Siemens Healthcare GmbH, Forchheim, Germany) operating in the dual-energy scan mode with the following scan parameters: tube A with a tin (Sn) filter, tube A voltage 140 kVp yielding an effective 60 mA, tube B voltage 80 kVp yielding an effective 141 mA, gantry rotation speed 0.28 s per rotation, collimation 64 × 0.5 mm, and pitch 1.00. Automatic tube current modulation (CareDose4D; Siemens Healthcare GmbH) was enabled.

We scanned all patients in the pulmonary arterial phase to minimize the influence of the systemic collateral supply [22]. Contrast medium containing 350 mg/mL iodine was administered at 0.075 mL/s/kg body weight over a period of 6 s, followed by a 40-mL saline flush delivered via a 20-gauge intravenous catheter placed in the right antecubital vein using the aid of a double-headed power injector (Dual Shot-Type GX; Nemoto-Kyorindo, Tokyo, Japan). The scan delay was determined using a test injection technique: 12 mL iodine-containing contrast medium followed by 20 mL normal saline. A region of interest (ROI) was placed within each main pulmonary artery, and the time-density curve within the ROI was recorded. The DE-CT scan commenced 1 s after test injection-mediated enhancement peaked. To reduce streak artifacts from dense contrast media in the superior vena cava or right atrium, images of the whole chest were acquired in a feet-to-head direction during a single inspirational breath-hold.

Both the low- and high-voltage spiral data were reconstructed at a thickness of 1 mm using 1-mm increments in the axial plane. To this end, we employed a medium-soft convolution kernel optimized for analysis of dual-energy images (D30f). Two image datasets were generated. First, mixed images obtained using a single energy of 120 kV were created by fusing the high- and low-voltage images using the aid of dual-energy application software on a commercially available workstation (syngo CT Workplace,

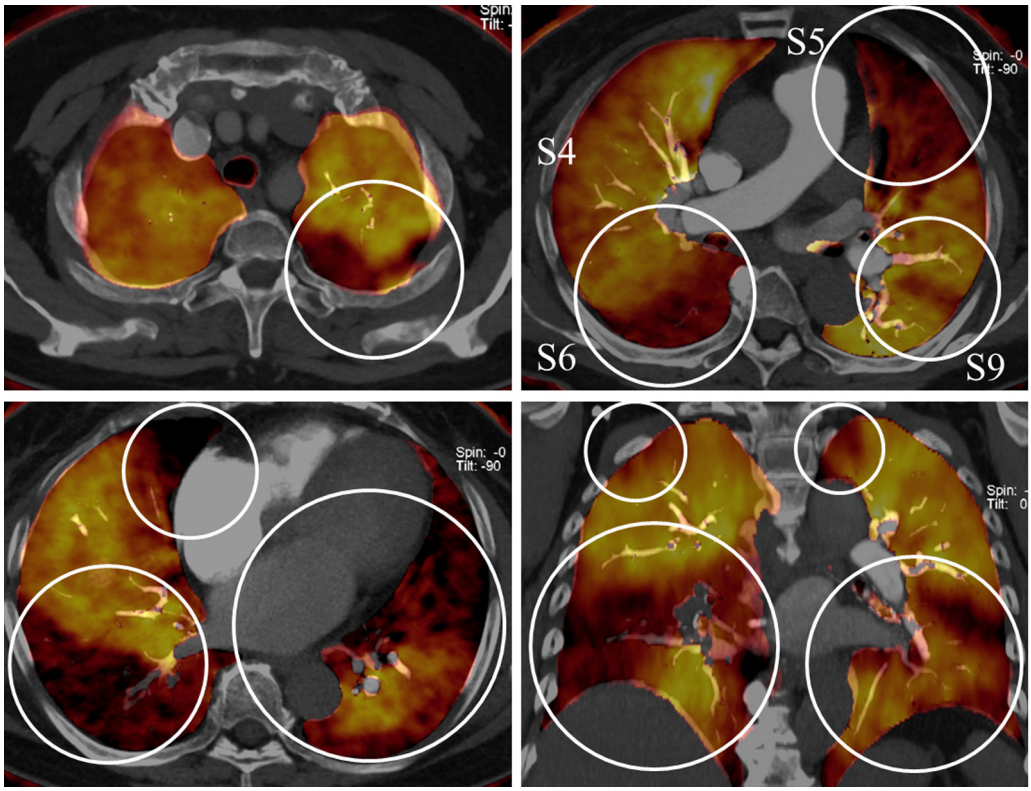

Fig. 1. A 72-year-old woman with CTEPH . In the lung PBV images, areas colored yellow or bright orange are normoperfused, and those colored dark orange or black are hypoperfused. Perfusion defects are evident peripherally in both lungs (the white circles). No perfusion defect (score 0) was evident in the right S4, a less-than-half perfusion defect in the left S9 (score 1), and a more-than-half perfusion defect in the left S5 (score 2). The lung PBV score (the sum of the scores of all segments) of this case was 22.

VA44A; Siemens Healthcare GmbH). Next, color-coded lung PBV Images 5-mm in thickness were reconstructed at 5-mm intervals in both the axial and coronal planes using the same dual-energy application software. The parameter default settings suggested by the manufacturer were employed. Thus, an ROI 0.5 cm^2 in area was placed in the pulmonary trunk; this was the reference vessel employed to calibrate the color-coding. The air density was set to −1000 HU on both the 80 kV and 140 kV (Sn) images; the soft tissue density was set to 60 HU on the 80 kV images and to 55 HU on the 140 kV (Sn) images; the contrast medium ratio was set to 3.01, the minimum border to −960 HU, the maximum border to −300 HU, the range to 5, and the contrast medium cutoff to −50 HU; all of these parameters were maintained in the factory default settings except for the following two parameters: the maximum border to include parenchymal regions with elevated CT values due to gravity-dependent opacity and/or insufficient maximal inspiratory scanning, and the range to reduce the graininess of the image appearance.

All adverse events associated with DE-CT examination were recorded and reviewed retrospectively. Both the volumetric CT dose index ($CTDI_{vol}$) and the dose-length product (DLP) were recorded for each patient. The corresponding effective radiation dose was calculated using a standard conversion factor for chest CT; this was 0.0145 mSv/mGy cm [23].

2.3. Image analysis

Two radiologists (one board-certified and one not) with 13 and 5 years of experience, respectively, blinded to the patient demographic and clinical information, independently scored the extent of perfusion defects in each lung segment using a 3-point scale (0, no defect, 1, defect in less than half the volume of a segment, 2, defect in more than half the volume of a segment), using both the axial and coronal color-coded lung PBV images (Fig. 1). On these images, areas that were black or dark orange were considered to be hypoperfused and areas that were bright orange or yellow to be normoperfused (Fig. 1). Artifacts caused by cardiac motion or the presence of the iodine contrast agent in the superior vena cava and/or right atrium constitute pseudo-perfusion defects evident on lung PBV images [20]. Both readers carefully identified and discounted such artifacts. In cases of disagreement, a final consensus was attained by discussion. The final lung PBV score was the sum of the scores of the 18 lung segments (Fig. 1); this score was calculated for all 46 patients. To explore possible non-uniformity of iodine-mediated lung parenchymal enhancement, the mean segment defect score was compared with those of the upper and lower regions of both lungs. The right upper part included five segments in the right upper and middle lobes, and the right lower part included five segments in the right lower lobe. The left upper part included four segments in the left upper lobe, and the left lower part included four segments in the left lower lobe.

To assess the severity of pulmonary hypertension, a single radiologist calculated the PA/Ao ratios by CT angiography. Vessel diameters were measured at the level of the principal PA bifurcation on the plane perpendicular to the course of each vessel. The mean CT values at the same levels of the principal PA and the descending aorta (dAo) were documented. ROIs were manually positioned at the centers of vessels evident on axial mixed images. All ROIs of the PA and dAo were greater than 100 mm^2 in area.

2.4. Assessment of clinical severity

6MWD data were obtained for 40 of the 46 patients, and BNP was recorded for all patients. Parameters measured via RHC examination included the PAP (systolic, diastolic, and mean), systolic right ventricular pressure (RVP), right atrial pressure (RAP),

cardiac output (CO), cardiac index (CI), and pulmonary capillary wedge pressure (PCWP). The PVR was calculated using the following formula: PVR = (mean PAP − PCWP)/CO × 80 (dyne s cm^{-5}). The systolic RVP was recorded for 42 of the 46 patients. All clinical and RHC-associated parameters were measured within 2 weeks of DE-CT examination (median: 1 day; range, 0–12 days). No patient exhibited symptom changes in the interval between CT and any other clinical examination, although all medications were maintained. No patient underwent either surgical or endovascular intervention during the between-test intervals.

2.5. Statistical analysis

Descriptive statistics are presented as means with standard deviations for normally distributed variables, as medians with interquartile ranges for non-normally distributed variables, and as numbers of cases (and percentages) per group for categorical variables. Within-subject variables were compared using the paired *t*-test or the Wilcoxon signed-rank test. Interobserver agreement of perfusion defect scoring per segment was evaluated by weighted Cohen's kappa values. To accommodate the use of multiple segments per patient, the weighted kappa values with 95% CIs were calculated using a bootstrap method (10,000 samples). Correlations between lung PBV score and the PA/Ao ratio, on the one hand, and the 6MWD, BNP level, and RHC-derived data, on the other, were evaluated by Spearman's rho correlation coefficients. Multivariable linear regression analyses using a stepwise method were used to explore whether noninvasive parameters were associated with the mean PAP and PVR. Non-normally distributed variables were subjected to $\log_{10}$-transformation prior to inclusion in the models. A p value < 0.05 was considered to indicate statistical significance. All computations were performed using the aid of JMP Pro 11 (SAS Institute Inc., Cary, NC, USA) and R3.1.3 (R Foundation for Statistical Computing, Vienna, Austria) software.

3. Results

All DE-CT examinations were successful, and no adverse events were noted. All patients exhibited good pulmonary arterial enhancement (mean CT value of the PA, 427 ± 117 HU) with less systemic arterial enhancement (mean CT value of the dAo, 108 ± 44 HU). The mean PA CT value was significantly higher than that of the dAo in all patients ($p < 0.01$). The mean $CTDI_{vol}$ and DLP values were 5.4 ± 1.1 mGy and 161 ± 35 mGy cm, respectively, and the mean effective radiation dose was 2.3 ± 0.5 mSv.

The extent of interobserver agreement in terms of perfusion defect scoring within each segment was excellent (bootstrapped weighted κ value = 0.88, 95% CIs: 0.85, 0.91). All patients exhibited abnormal (bilateral) lung perfusion; the median lung PBV score was 17 (25th percentile 12, 75th percentile 20, [range] 5–27). The distributions of the mean defect scores within each lung segment are summarized in Fig. 2. The mean defect scores were as follows: right upper part 1.11 (95% CIs: 0.90, 1.23); right lower part 0.81 (95% CIs: 0.60, 0.94); left upper part 0.93 (95% CIs: 0.79, 1.07); and left lower part 0.64 (95% CIs: 0.50, 0.77). The upper parts of both lungs had significantly higher PBV scores than those of the lower parts ($p < 0.01$ for both lungs). The mean principal PA diameter was 31.4 ± 3.7 mm, and the mean PA/Ao ratio was 0.98 ± 0.15. The results of the 6MWD and BNP evaluations, the RHC-derived data, and the correlations between the CT findings and these other measures of clinical severity are summarized in Table 2. Twenty-eight (61%) patients had mean PAP values < 25 mmHg, because they had undergone prior surgical or endovascular interventions. Moderately positive correlations between the lung PBV and systolic PAP, diastolic PAP, mean PAP, systolic RVP, and PVR were evident ($p < 0.01$ for all comparisons) (Fig. 3). We found no significant correlation between the lung PBV score and either the 6MWD, BNP, CO, or CI. The PA/Ao ratio was mildly-to-moderately (positively) correlated with the systolic PAP, diastolic PAP, mean PAP, and RVP. No significant correlation between the PA/Ao ratio and either the 6MWD, BNP level, or PVR was evident.

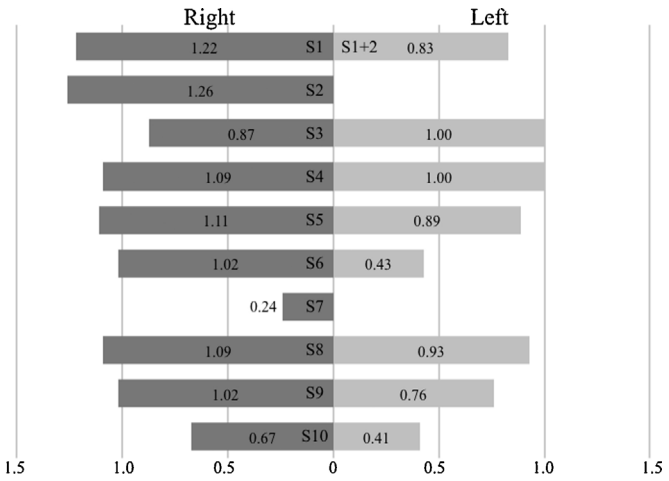

Fig. 2. The mean perfusion defect scores of each segment. The upper parts of both lungs had significantly higher PBV scores than those of the lower parts (right lung 1.11 vs. 0.81, left lung 0.93 vs. 0.64, respectively; $p < 0.01$ for both comparisons).

The BNP levels were $\log_{10}$-transformed prior to multivariable linear regression analyses. Such analyses were performed in 40 patients who had available data on CT, RHC-derived, and clinical parameters. Among the independent variables, only the lung PBV score (coefficient, 28.83, 95% CIs: 13.3, 44.28, $p < 0.01$) was significantly associated with the PVR. Log_{10}-transformed BNP (coefficient, 7.53, 95% CIs: 2.15, 12.91, $p < 0.01$) and lung PBV scores (coefficient, 0.84, 95% CIs: 0.32, 1.37, $p < 0.01$) were significantly associated with the mean PAP.

4. Discussion

We found that the extent of pulmonary hypoperfusion in the pulmonary arterial phase, as evaluated by calculating lung PBV scores, was positively correlated with the systolic RVP, PAP, and PVR. Furthermore, the lung PBV score was the only parameter to exhibit a significant association with both the mean PAP and PVR, among both CT and other noninvasive parameters. The mean PAP and PVR as measured by RHC are useful estimators of long-term prognosis [5,6] and are commonly employed to measure the severity of CTEPH . Although RHC remains the gold standard for diagnosis and evaluation of CTEPH, noninvasive estimation of disease severity using lung PBV scores will be valuable, particularly to reduce the need for repeat RHC procedures during long-term follow-up. CTPA combined with lung PBV is accurate when used to diagnose CTEPH (sensitivity, 100%, specificity, 92%) [24]. However, measurement of the clinical severity of disease by calculation of lung PBV will enhance the utility of CT when managing patients with CTEPH .

Hoey et al. evaluated the correlation between visual lung PBV findings and clinical measures of CTEPH severity [20]. In the cited study, the visual perfusion impairment score did not correlate significantly with the mean PAP or PVR [20]. This discrepancy (compared with what we found) may be explained by the different scan delays used. The scan delay of the cited work was 7 s after pulmonary trunk peak enhancement, in contrast to the 1 s of our study; 85% of patients in the cited study exhibited good systemic arterial enhancement. CTEPH patients develop extensive collateral supply

Table 2
Results of clinical severity parameters and correlation with lung PBV score and PA/Ao ratio.

Parameters	Median (range)	Lung PBV score Spearman's rho (95% CI)	*P*-value	PA/Ao ratio Spearman's rho (95% CI)	*P*-value
6MWD (m)	487 (90–673)	−0.26 (−0.43, −0.10)	=0.11	0.02 (−0.14, 0.18)	=0.93
BNP (pg/ml)	34.2 (5.8–560.0)	0.27 (0.12, 0.43)	=0.68	0.13 (−0.02, 0.28)	=0.40
Systolic PAP (mmHg)	41 (29–98)	0.47 (0.36, 0.66)	<0.01*	0.31 (0.17, 0.47)	=0.036*
Diastolic PAP (mmHg)	15 (5–34)	0.39 (0.26, 0.56)	<0.01*	0.41 (0.28, 0.59)	<0.01*
Mean PAP (mmHg)	24 (15–52)	0.48 (0.37, 0.68)	<0.01*	0.39 (0.24, 0.54)	<0.01*
Systolic RVP (mmHg)	42 (28–98)	0.48 (0.36, 0.68)	<0.01*	0.41 (0.28, 0.60)	<0.01*
RAP (mmHg)	5 (0–16)	0.08 (−0.07, 0.23)	=0.60	0.21 (0.06, 0.37)	=0.16
CO (l/min)	3.95 (1.82–6.22)	−0.10 (−0.25, 0.05)	=0.50	0.18 (0.03, 0.33)	=0.23
CI (l/min/m^2)	2.58 (1.21–3.68)	−0.13 (−0.28, −0.02)	= 0.38	0.12 (−0.03, 0.27)	=0.39
PVR (dyne s cm^{-5})	267 (110–1450)	0.47 (0.36, 0.66)	<0.01*	0.25 (0.10, 0.41)	=0.10

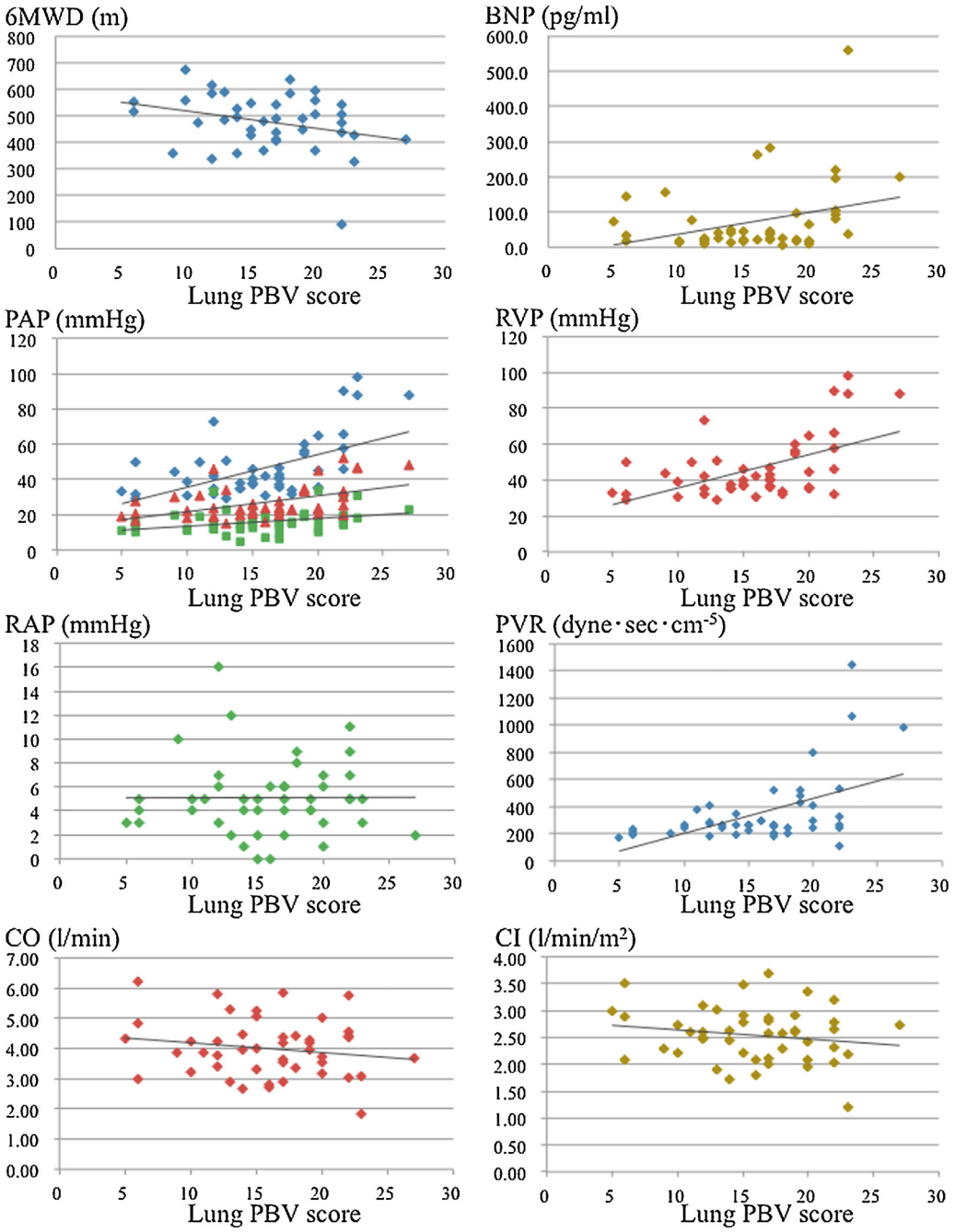

Fig. 3. Correlations between lung PBV scores and other clinical parameters. Moderate positive correlations were evident between the lung PBV score and the systolic PAP, diastolic PAP, mean PAP, systolic RVP, and PVR ($p < 0.01$ for all comparisons). No significant correlation was evident with any other parameter.

networks from the systemic arterial system, which may cause the extent of pulmonary hypoperfusion to be underestimated upon lung PBV evaluation [22,25–27]. Therefore, we employed a shorter scan delay; all patients exhibited slight systemic arterial enhancement but significantly higher PA enhancement (mean CT values, 427 ± 117 HU [PA] vs. 108 ± 44 HU, respectively, $p < 0.01$). Therefore, lung PBV during the pulmonary arterial phase minimizes the influence of the collateral systemic supply, and the data correlate better with other severity parameters. A potential drawback of our protocol may be that the brief scan delay is associated with a risk that the contrast medium may not include the lung parenchyma. If the scan delay were in fact too short, the lower parts of the lungs would be more obviously hypoperfused compared with the upper parts when the scan direction is feet-to-head. However, we found that the defect scores of the lower parts of the lungs were in fact lower than those of the upper parts. Therefore, our protocol may in fact be optimal.

Meinel et al. correlated automatically calculated lung PBV measurements with the PAP, PVR, CI, and 6MWD in 25 CTEPH patients [21]. Although their data are in partial agreement with ours, the limited statistical power of the cited work resulted in a significant correlation only between the lung PBV and PAP [21]. The advantages of automated quantification include reader-independence and speed. However, when used to calculate lung PBVs, such quantification misinterprets artifacts caused by cardiac motion or the iodine contrast medium. Therefore, we preferred visual evaluation; we manually measured pulmonary perfusion while carefully discounting artifacts. Although visual assessment is reader-dependent, our interobserver agreement was excellent (bootstrapped weighted $\kappa = 0.88$, 95% CIs, 0.85, 0.91).

An earlier report found a significant correlation between the PA/Ao ratio and PAP [28]; we thus evaluated the PA/Ao ratio as a potentially noninvasive estimator of the severity of CTEPH. We considered that PA dilatation had developed secondarily to long-standing pulmonary hypertension. However, age, sex, and other cardiopulmonary conditions may confound PA and Ao data [29]. Although a significant (albeit moderate) correlation was evident between the PA/Ao ratio and PAP, multiple regression analysis showed that the lung PBV score was a stronger estimator of disease than was either the PA/Ao ratio or any other noninvasive parameter.

Our study had several limitations. First, 27 of the 46 (58.7%) patients had mean PAPs < 25 mmHg because they had been treated for CTEPH before their enrollment. In the European and American guidelines, pulmonary hypertension is defined by a resting mean PAP $\geq$ 25 mmHg [14,30]. However, the upper level of normal for the resting mean PAP is considered 20 mmHg, and a mean PAP between 21 and 24 mmHg is considered borderline pH [30]. Among the 27 patients, 23 (85.1%) had a mean PAP > 20 mmHg, and 4 patients had mean PAPs between 15 and 20 mmHg and elevated PVR (>240 dyne s cm^{-5}). Therefore, all of the patients in our study had pathophysiological conditions in the pulmonary circulation caused by CTEPH . Although we assume that the PAP and PVR improvements evident after the earlier interventions were attributed to (some) recanalization of the pulmonary arteries, further evaluation of correlations between lung PBV or the PA/Ao ratio and the clinical severity of disease before and after intervention is warranted. Enrollment of medication-naïve patients was not possible; diagnosis required the use of medication to distinguish CTEPH from an acute or subacute pulmonary embolism. Second, our scoring did not consider volume differences among lung segments. In addition, although we evaluated lung PBV based on the extent of pulmonary hypoperfusion, we did not consider regional reductions in perfusion. We categorized both severely affected (black) and moderately affected (dark orange) areas as simply “hypoperfused”. However, our scoring system may be clinically useful because the inter-reader agreement is excellent.

5. Conclusions

The lung PBV score is a noninvasive estimator of the clinical severity of CTEPH than is calculation of the mean PAP and PVR values; these latter values currently serve as the gold standards for management of the condition.

Conflict of interest

The second author (H.O.) received a grant support by the Clinical Research Promotion Program for Young Investigators of Tohoku University Hospital and Grant-in-Aid for Scientific Research (C) grant number JP16K10265 for this study. The fourth author (K.O.) is an employee of Diagnostic Imaging Business Area, DI Research & Collaboration Department, Siemens Healthcare KK. Although she had no input into image analysis, she made substantial contribution to the conception and design of the study, revising the article and final approval of the version. The other authors declare no conflicts of interest.

Role of the funding source

This work was supported by the Clinical Research Promotion Program for Young Investigators of Tohoku University Hospital and Grant-in-Aid for Scientific Research (C) grant number JP16K10265.

References

[1] V. Pengo, A.W.A. Lensing, M.H. Prins, A. Marchiori, B.L. Davidson, F. Tiozzo, et al., Incidence of chronic thromboembolic pulmonary hypertension after pulmonary embolism, N. Engl. J. Med. 350 (2004) 2257–2264.
[2] C. Becattini, G. Agnelli, R. Pesavento, M. Silingardi, R. Poggio, M.R. Taliani, et al., Incidence of chronic thromboembolic pulmonary hypertension after a first episode of pulmonary embolism, Chest 130 (2006) 172–175.
[3] G. Simonneau, M.A. Gatzoulis, I. Adatia, D. Celermajer, C. Denton, A. Ghofrani, et al., Updated clinical classification of pulmonary hypertension, J. Am. Coll. Cardiol. 62 (2013) 34–41.
[4] G. Piazza, S.Z. Goldhaber, Chronic thromboembolic pulmonary hypertension, N. Engl J. Med. 364 (2011) 351–360.
[5] M. Riedel, V. Stanek, J. Widimsky, I. Prerovsky, Longterm follow-up of patients with pulmonary thromboembolism. Late prognosis and evolution of hemodynamic and respiratory data, Chest 81 (1982) 151–158.
[6] J. Lewczuk, P. Piszko, J. Jagas, A. Porada, S. Wójciak, B. Sobkowicz, et al., Prognostic factors in medically treated patients with chronic pulmonary embolism, Chest 119 (2001) 818–823.
[7] E. Mayer, D. Jenkins, J. Lindner, A. D'Armini, J. Kloek, B. Meyns, et al., Surgical management and outcome of patients with chronic thromboembolic pulmonary hypertension: results from an international prospective registry, J. Thorac. Cardiovasc. Surg. 141 (2011) 702–710.
[8] K. Sugimura, Y. Fukumoto, K. Satoh, K. Nochioka, Y. Miura, T. Aoki, et al., Percutaneous transluminal pulmonary angioplasty markedly improves pulmonary hemodynamics and long-term prognosis in patients with chronic thromboembolic pulmonary hypertension, Circ. J. 76 (2012) 485–488.
[9] H.J. Reesink, M.N. van der Plas, N.E. Verhey, R.P. van Steenwijk, J.J. Kloek, P. Bresser, Six-minute walk distance as parameter of functional outcome after pulmonary endarterectomy for chronic thromboembolic pulmonary hypertension, J. Thorac. Cardiovasc. Surg. 133 (2007) 510–516.
[10] H.J. Reesink, I.I. Tulevski, J.T. Marcus, F. Boomsma, J.J. Kloek, A.V. Noordegraaf, et al., Brain natriuretic peptide as noninvasive marker of the severity of right ventricular dysfunction in chronic thromboembolic pulmonary hypertension, Ann. Thorac. Surg. 84 (2007) 537–543.
[11] M.M. Redfield, R.J. Rodeheffer, S.J. Jacobsen, D.W. Mahoney, K.R. Bailey, J.C. Burnett Jr., Plasma brain natriuretic peptide concentration: impact of age and gender, J. Am. Coll. Cardiol. 40 (2002) 976–982.
[12] N.H. Kim, M. Delcroix, D.P. Jenkins, R. Channick, P. Dartevelle, P. Jansa, et al., Chronic thromboembolic pulmonary hypertension, J. Am. Coll. Cardiol. 62 (2013) 92–99.
[13] M.M. Hoeper, S.H. Lee, R. Voswinckel, M. Palazzini, X. Jais, A. Marinelli, et al., Complications of right heart catheterization procedures in patients with pulmonary hypertension in experienced centers, J. Am. Coll. Cardiol. 48 (2006) 2546–2552.
[14] N. Galiè, M. Humbert, J.-L. Vachiery, S. Gibbs, I. Lang, A. Torbicki, et al., ESC/ERS Guidelines for the diagnosis and treatment of pulmonary

hypertension: The Joint Task Force for the Diagnosis and Treatment of Pulmonary Hypertension of the European Society of Cardiology (ESC) and the European Respiratory Society (ERS)Endorsed by: Association for European Paediatric and Congenital Cardiology (AEPC), International Society for Heart and Lung Transplantation (ISHLT), Eur. Heart J. 46 (2015) 903–975.
[15] A. Reichelt, M.M. Hoeper, M. Galanski, M. Keberle, Chronic thromboembolic pulmonary hypertension: evaluation with 64-detector row CT versus digital substraction angiography, Eur. J. Radiol. 71 (2009) 49–54.
[16] T. Sugiura, N. Tanabe, Y. Matsuura, A. Shigeta, N. Kawata, T. Jujo, et al., Role of 320-slice CT imaging in the diagnostic workup of patients with chronic thromboembolic pulmonary hypertension, CHEST J. 143 (2013) 1070–1077.
[17] T.R.C. Johnson, C. Fink, S.O. Schönberg, M.F. Reiser, Dual Energy in Clinical Practice, 1st ed., Springer Berlin Heidelberg, New York, 2011.
[18] T. Nakazawa, Y. Watanabe, H. Yoshiro, K. Keisuke, H. Masahiro, N. Hiroaki, Lung perfused blood volume images with dual-energy computed tomography for chronic thromboembolic pulmonary hypertension: correlation to scintigraphy with single-photon emission computed tomography, J. Comput. Assist. Tomogr. 35 (2011) 591–595.
[19] N. Galiè, N.H.S. Kim, Pulmonary microvascular disease in chronic thromboembolic pulmonary hypertension, Proc. Am. Thorac. Soc. 3 (2006) 571–576.
[20] E.T.D. Hoey, S. Mirsadraee, J. Pepke-Zaba, D.P. Jenkins, D. Gopalan, N.J. Screaton, Dual-energy CT angiography for assessment of regional pulmonary perfusion in patients with chronic thromboembolic pulmonary hypertension: initial experience, Am. J. Roentgenol. 196 (2011) 524–532.
[21] F. Meinel, A. Graef, K. Thierfelder, M. Armbruster, C. Schild, C. Neurohr, et al., Automated quantification of pulmonary perfused blood volume by dual-energy CTPA in chronic thromboembolic pulmonary hypertension, RöFo—Fortschritte Auf Dem Geb. Röntgenstrahlen Bildgeb. Verfahr. 186 (2013) 151–156.
[22] Y.J. Hong, J.Y. Kim, K.O. Choe, J. Hur, H.-J. Lee, B.W. Choi, et al., Different perfusion pattern between acute and chronic pulmonary thromboembolism: evaluation with two-phase dual-energy perfusion CT, Am. J. Roentgenol. 200 (2013) 812–817.
[23] P.D. Deak, Y. Smal, W.A. Kalender, Multisection CT protocols: sex-and age-specific conversion factors used to determine effective dose from dose-length product, Radiology 257 (2010) 158–166.
[24] G. Dournes, D. Verdier, M. Montaudon, E. Bullier, A. Rivière, C. Dromer, et al., Dual-energy CT perfusion and angiography in chronic thromboembolic pulmonary hypertension: diagnostic accuracy and concordance with radionuclide scintigraphy, Eur. Radiol. 24 (2014) 42–51.
[25] S. Ley, K.-F. Kreitner, I. Morgenstern, M. Thelen, H.-U. Kauczor, Bronchopulmonary shunts in patients with chronic thromboembolic pulmonary hypertension: evaluation with helical CT and MR imaging, Am. J. Roentgenol. 179 (2002) 1209–1215.
[26] M. Remy-Jardin, A. Duhamel, V. Deken, N. Bouaziz, P. Dumont, J. Remy, Systemic collateral supply in patients with chronic thromboembolic and primary pulmonary hypertension: assessment with multi-detector row helical CT angiography, Radiology 235 (2005) 274–281.
[27] B. Renard, M. Remy-Jardin, T. Santangelo, J.-B. Faivre, N. Tacelli, J. Remy, et al., Dual-energy CT angiography of chronic thromboembolic disease: can it help recognize links between the severity of pulmonary arterial obstruction and perfusion defects? Eur. J. Radiol. 79 (2011) 467–472.
[28] A. Mahammedi, A. Oshmyansky, P.M. Hassoun, D.R. Thiemann, S.S. Siegelman, Pulmonary artery measurements in pulmonary hypertension: the role of computed tomography, J. Thorac. Imaging 28 (2013) 96–103.
[29] Q.A. Truong, J.M. Massaro, I.S. Rogers, A.A. Mahabadi, M.F. Kriegel, C.S. Fox, et al., Reference values for normal pulmonary artery dimensions by noncontrast cardiac computed tomography the framingham heart study, Circ. Cardiovasc. Imaging 5 (2012) 147–154.
[30] M.M. Hoeper, H.J. Bogaard, R. Condliffe, R. Frantz, D. Khanna, M. Kurzyna, et al., Definitions and diagnosis of pulmonary hypertension, J. Am. Coll. Cardiol. 62 (2013).